High-resolution frequency standard at 1030 nm for Yb:YAG solid-state lasers

Jun Ye, Long-Sheng Ma,* and John L. Hall

JILA, National Institute of Standards and Technology and University of Colorado at Boulder, Boulder, Colorado 80309-0440

Received January 3, 2000; revised manuscript received March 20, 2000

A diode-pumped solid-state Yb:YAG laser has been stabilized to a high-finesse cavity with an all-external servo loop. Ultrasensitive cavity-enhanced frequency modulation spectroscopy has recovered a sub-Doppler acetylene overtone transition with a high signal-to-noise ratio, leading to an absorption sensitivity of 7×10^{-11} at a 1-s averaging time. This high-resolution molecular resonance serves as a long-term stable reference for the laser. The system can be developed into a highly compact and stable optical frequency standard in the 1.03-μm wavelength range. © 2000 Optical Society of America [S0740-3224(00)03206-9]

OCIS codes: 140.3580, 140.0140, 300.6360, 300.6390, 300.6460, 350.4800.

Diode-pumped solid-state lasers are viewed as the most promising coherent light sources in many different application fields that include communications, remote sensing and detection, high-resolution spectroscopy, and precision measurement. Aside from their demonstrated merits in the areas such as energy efficiency, size, lifetime, and intrinsic noise levels, new solid-state laser systems that cover different wavelength ranges are under active development. Diode-pumped Yb:YAG lasers offer certain advantages over lasers such as those with Nd:YAG, in terms of low thermal load, long upper-state lifetime, absence of excited-state absorption and upconversion loss, and a wide absorption band at 940 nm that is within the InGaAs diode laser emission range. Yb:YAG is thus a better candidate for high-power and high-efficiency laser operation.[1] Yb:YAG also offers a broad emission spectrum that supports femtosecond pulse generation.[2] In the cw world, tunable sources at 1.03 (and 1.05) μm are of course welcome for spectroscopy work. However, the lack of a suitable reference in this wavelength region has limited the laser in certain applications in which precise knowledge of its frequency or wavelength is required. In this paper we report, for the first time to our knowledge, a high-resolution (sub-Doppler molecular vibration overtone transition) frequency reference around 1.03 μm for the Yb:YAG laser.

The tunable Yb:YAG laser[3] employed in our experiment outputs 50 mW (of a single-longitudinal mode) near 1030 nm with 800 mW of diode pump power. The laser wavelength can be tuned slowly only with a temperature control of its resonator. Therefore, to achieve frequency stabilization of the laser with a reasonably wide bandwidth, a frequency- and phase-correcting transducer external to the laser is needed.[4] An acousto-optic modulator (AOM) is used for this purpose. The free-running laser linewidth is of the order of 20 kHz at measurement times below 0.1 ms. However, to establish effective long-term frequency stabilization by use of a natural atomic or molecular reference, this fast laser linewidth needs to be reduced further, to a level at which the resonance information can be recovered with an enhanced signal-to-noise (S/N) ratio and used efficiently to suppress the laser frequency jitter and drift. In other words, when a local oscillator is more stable, it can afford to spend a longer time for its frequency and phase to evolve on its own before having to make an inquiry about the reference. This longer interrogation period translates into a smaller bandwidth for both the resonance signal recovery process (and thus a finer examination of the true line center) and the long-term servo loop that locks the laser frequency onto the resonance. For the purpose of short-term stabilization of the laser, an optical cavity is often utilized.[5] In our previous study of ultrasensitive cavity-enhanced frequency modulation (FM) spectroscopy[6] we combined the operations of long- and short-term stabilization into one apparatus, with the information of the cavity resonance and of the intracavity molecular transition being made available to the laser simultaneously. We follow the same strategy in the present work.

The whole setup of the Yb:YAG laser frequency stabilization is illustrated in Fig. 1. Electro-optic modulator 1 (EOM 1) allows the frequency and phase of the optical field (relative to the cavity) to be sampled at 4 MHz. Phase-coherent demodulation of the cavity-reflected light (photodetector 1) at this carrier frequency reveals the servo error signal that is to be used for locking the laser onto the cavity mode. The external AOM can be used for both frequency and intensity stabilization. Since the temperature response of the laser resonator is limited to a time constant of ~1 s, we need to extend the frequency servo gain of the AOM basically to the dc range. (In a more typical case a laser resonator would have some sort of mechanical tuning capability enabled, for example, by a piezoelectric transducer (PZT) mounted on one of the mirrors. We would then roll off the gain of the AOM at low frequency ranges so that the PZT will be chiefly responsible to correct any slow but potentially large frequency noise of the laser.[7]) To avoid the excessive beam pointing noise, we adopt a double-passing scheme for the AOM so that the diffracted beam from the AOM does not have a

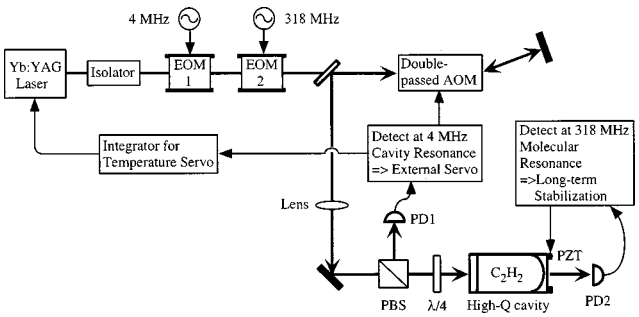

Fig. 1. Frequency stabilization of a Yb:YAG laser by use of an optical resonator with intracavity molecular absorption. The information about the resonance of the cavity (molecule), the so-called error signal, is recovered by phase-coherent detection of the cavity-reflected (transmitted) light at 4 MHz (318 MHz). PBS, polarized beam splitter; PD, photodetector. EOM, electro-optic modulator.

pointing-direction dependence on the AOM drive frequency.

The cavity has a free-spectral-range frequency of 318.34 MHz. The cavity field ring-down time ($1/e$) is measured to be 75 μs, leading to a cavity linewidth (FWHM) of 4.3 kHz and a finesse of 75,000 at 1.03 μm. The cavity-locking signal is derived from the heterodyne beat between the field of direct reflection off the input mirror and the leakage of the cavity-stored field via the input mirror. Therefore the error contains frequency information on time scales longer than the cavity response time but phase information on shorter time scales. The narrow cavity linewidth does not limit the available servo bandwidth but instead aids in the measurement efficiency of frequency and phase noise. In the design of the servo loop filter function we first compensate for the cavity response with an electronic transfer function that has a pole at dc and a zero at the cavity bandwidth. The combined response of the cavity and this first-stage amplifier is a net integrator (for frequency errors) over the whole relevant frequency range. With a predetermined knowledge of a 400-ns time delay (which is due to the propagation of the sound wave through the optical beam inside the crystal) of the AOM that is used for frequency correction, the loop is optimized with a unity gain bandwidth of 150 kHz. A second-stage integrator is used below 1 kHz to provide more gain at low-frequency ranges, where the frequency noise of the laser strongly increases. The output of the loop filter feeds a voltage-controlled oscillator (VCO) that drives the AOM. To prevent saturation of the VCO control signal, it is integrated one more time and is fed to the laser resonator temperature servo, with a crossover frequency of ~0.1 Hz between the VCO and the thermal controls.

Figure 2 shows the in-loop error signal analysis for the case in which the laser is locked to the cavity. The noise spectrum of the signal on a radio-frequency (rf) spectrum analyzer reveals a servo noise bump near the unity gain frequency of 150 kHz [Fig. 2(a)]. At the lower-frequency range a fast-Fourier-transform (FFT) analyzer gives a more accurate measurement of the noise spectrum with its finer resolution bandwidth. Figure 2(b) displays the signal analysis and comparison performed by the FFT analyzer (listed from bottom to top): electronic noise floor, shot noise, light noise, error signal under a tight-lock condition, and error signal under a loose-lock condition. The noise spectrum measured at the analyzer (in units of $V/Hz^{1/2}$) is converted to the frequency noise spectral density (in $Hz/Hz^{1/2}$), by means of the slope (Hz/V) of the discriminating error signal. At Fourier frequencies higher than the cavity response corner frequency, the low-pass behavior of the cavity $\{\sim|[1/(1 + jx)]|$, with x being the normalized frequency detuning from the cavity resonance$\}$ is taken into account by conversion of the phase noise spectrum into the frequency noise spectrum through division by this cavity response function. The white shot noise of the detector corresponds to white phase noise above the cavity corner frequency, therefore leading to rising frequency noise at higher Fourier frequencies. We can see that, although we modulate and demodulate the light at a high frequency (4 MHz), the light intensity noise is still ~3 dB above the shot-noise level (at a power of 0.3 mW at the detector). Under a tightly locked condition the in-loop error signal noise appears to be ~20 times above the measured shot-noise limit. So we are operating in the gain-limited domain, and the observed variations represent a close estimation of the actual laser noise. The maximum gain that we can employ is limited by the loop bandwidth, which is in turn limited by the AOM's time delay.

To determine the coherent linewidth of the laser, we convert the frequency spectral density to phase noise

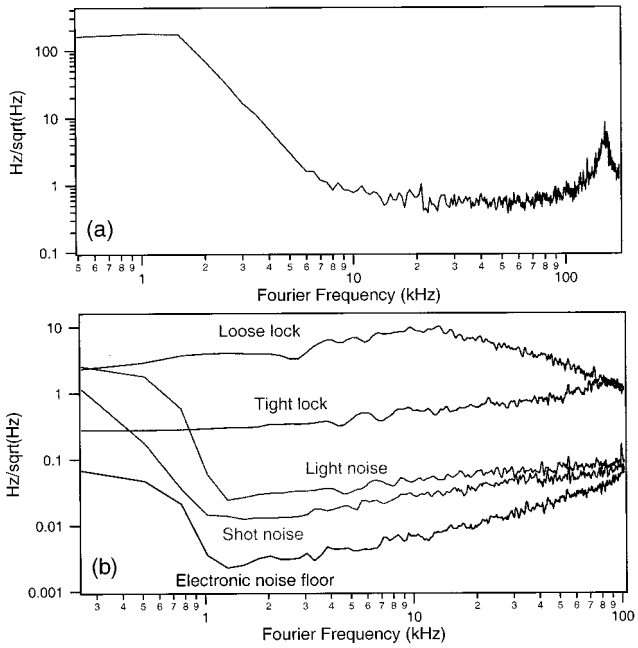

Fig. 2. In-loop error signal analysis under the locked condition. (a) Error signal analyzed by a rf spectrum analyzer, showing the servo noise bump near the unity gain frequency of 150 kHz. The rising noise level at low frequencies is due to the rf spectrum analyzer. (b) FFT analysis of the error signal under two locking conditions. Also shown are the base levels of electronic noise and light. The signals obtained directly from the detector contain information about both frequency noise (at Fourier frequencies below the cavity corner frequency) and phase noise (at Fourier frequencies above the cavity corner frequency). We have used the cavity response function to convert the phase noise into the corresponding frequency noise spectrum.

spectral density and calculate the accumulated rms phase variance. The first part of the integration is carried out from 1 MHz (where the measured noise approaches the shot-noise limit) to 10 kHz, with a resulting phase variance less than $3 \times 10^{-4}\,\mathrm{rad}^2$. This results from the fact that the fast frequency fluctuations have small phase modulation indices and consequently convert only a negligible portion of the carrier power to noise sidebands. Below 10 kHz the frequency noise spectral density ($\sqrt{S_f}$) is roughly flat at 0.3 $\mathrm{Hz/Hz^{1/2}}$. The small fluctuations lead to a 0.28-Hz laser linewidth relative to the cavity, given by[8] $\Delta\nu_{\mathrm{laser}} = \pi S_f$. When the feedback gain is turned down, the rapidly rising frequency noise of the laser at the low-frequency range certainly becomes visible.

In the case in which the gain of the feedback loop is sufficiently high one can totally suppress the original laser noise and can replace it with the measurement noise via the servo. In other words, $\sqrt{S_f} = \Delta\nu_{\mathrm{cavity}}/(S/N)$, where $\Delta\nu_{\mathrm{cavity}}$ is the cavity linewidth (HWHM) and S/N denotes the quality of the recovered information about cavity resonance. With the FM sideband technique the measurement noise can approach its minimum possible value, the fundamental shot-noise limit. Hils and Hall[9] derived a theoretical estimation of shot-noise-limited laser frequency noise spectral density under feedback:

$$S_f = (\Delta\nu_{\mathrm{cavity}})^2 \frac{1 - J_0^2(2\sqrt{T_{\mathrm{cavity}}} - T_{\mathrm{cavity}})}{T_{\mathrm{cavity}}} \frac{e}{4J_0^2 J_1^2 P \eta}. \tag{1}$$

Here the optical power $P = 0.3\,\mathrm{mW}$, the detector responsivity $\eta = 0.4$ A/W, the cavity's resonant transmission efficiency $T_{\mathrm{cavity}} = 20\%$, and $J_0 = 0.96$, $J_1 = 0.2$ (zero- and first-order Bessel functions) for a modulation index of 0.4 at 4 MHz. Based on these parameters, $\sqrt{S_f}$ is calculated to be 0.3 $\mathrm{mHz/Hz^{1/2}}$, ~1000 times smaller than the measured value. Improvement of the current system would require better optical isolation and a wider servo bandwidth.

Still, the laser's intrinsic noise below 100 kHz has been strongly reduced by the servo action. So we can conclude that most of the noise imposed on the VCO by the closed-loop feedback rather closely matches the laser's intrinsic noise. Thus information about the frequency noise of the free-running laser is readily available from the readout of the AOM–VCO. To establish a reference level the intrinsic noise of the VCO frequency is measured first, without laser–cavity locking. The added noise of the VCO when the AOM is used in the servo loop clearly reflects the relative noise between the laser and the cavity. To be able to estimate the laser's parameters we then need to consider the reference cavity's noise.

The cavity is located inside an evacuated chamber that provides both thermal and vibration isolation. However, the stability of the cavity is slightly degraded by the PZT-mounted mirrors, which are necessary to scan out the molecular resonance. We use a low-noise, high-voltage PZT driver of 5 $\mu\mathrm{V/Hz^{1/2}}$ noise density within a 60-Hz bandwidth.[10] Considering that the PZT scans through one cavity free spectral range (318.3 MHz) with 500 V, the added noise by the PZT driver is therefore estimated at 3 $\mathrm{Hz/Hz^{1/2}}$. When the cavity length is stabilized to a molecular transition, the bandwidth within which we use the PZT is of course eventually decided by the servo loop. Since the mode frequency of the passive cavity does not have much fast fluctuation and its long-term drift can be stabilized, the VCO noise can then be used to deduce the frequency noise of the free-running laser. Figure 3 compares the Allan variance of the counted VCO frequency under locked and free-running conditions. The figure shows that the intrinsic VCO frequency fluctuation is of the order of a few hundred hertz. However, when the laser is locked on the cavity, the VCO has to vary by a few kilohertz to a few tens of kilohertz so that the laser noise can be compensated for. At short time scales such as 1–10 μs the laser frequency noise is approximately $2 \times (10\text{–}30)$ kHz (the factor of 2 accounts for the fact that the AOM is double passed). The noise drops down to $2 \times (2\text{–}3)$ kHz at an averaging time of a few tens of milliseconds, and then the drift of the laser takes over for longer measurement times.

In terms of the coherent linewidth of the laser, we note that fast frequency fluctuations do not accumulate as much random phase noise as do the slow fluctuations. For example, 20-kHz frequency noise at 1 μs contributes a rms phase excursion of less than 1 rad. However, 10-kHz frequency noise at 1 ms causes a random phase excursion far bigger than 1 rad, and the definition of a coherent linewidth is no longer valid. According to Fig. 3, the (radian) breakpoint of the linewidth seems to be $\leqslant$0.1 ms, and the frequency noise there is $\sim 2 \times (10\text{–}20)$ kHz. We can verify this result, using a different measurement strategy. We directly compare the linewidth of the VCO itself under the locked and the free-running conditions. The nominal frequency of the VCO is 80 MHz, and it is downconverted with a frequency synthesizer to 50 kHz for FFT analysis. Figure 4 shows the dramatic change of the VCO linewidth for the case in which the feedback gain of the laser–cavity lock is increased from zero to maximum. This broadened linewidth of 20 kHz of the VCO carrier can be directly related to the linewidth of the original free-running laser ($\sim 2 \times 20$ kHz). The resolution bandwidth is 1 kHz, corresponding to an averaging time of 0.16 ms. Note that the power of the original VCO carrier

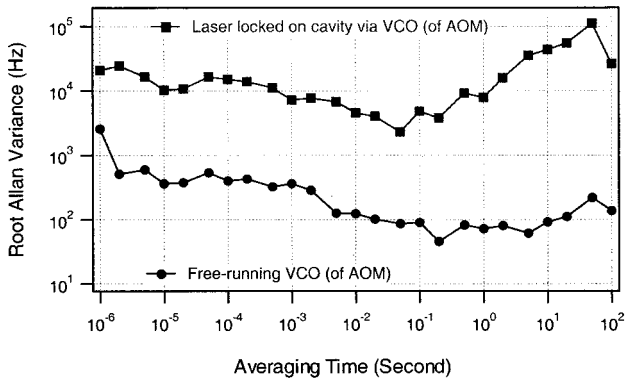

Fig. 3. Root Allan variance of the AOM–VCO frequency. The curve with circles represents the VCO frequency noise under the free-running condition. The curve with squares shows the increased VCO frequency noise for the case in which the VCO is being used in the servo to correct the laser frequency noise. The difference between the two curves indicates a direct measurement of the laser frequency noise.

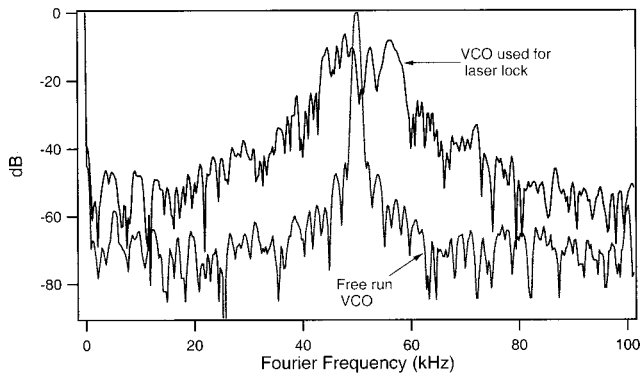

Fig. 4. Comparison of the VCO linewidth under the locked and the free-running conditions. The 80-MHz VCO frequency is mixed down to 50 kHz for FFT analysis at a 1-kHz resolution bandwidth. The original VCO linewidth is not resolved by the 1-kHz bandwidth. When the VCO is used to lock the laser to the cavity, the linewidth increases to ~20 kHz.

drops, owing to the loss of its energy into the phase noise fluctuations that the VCO makes to compensate for the laser noise.

Long-term stabilization of this laser–cavity system is provided by the acetylene molecules filled inside the cavity. The transition involved is a vibration overtone line[11]: $C_2H_2(3\nu_3)R(29)$, located at 1031.6528 nm, with a transition dipole moment of 0.59 mD (1 debye $= 3.33564 \times 10^{-30}$ C m). For the purpose of high-resolution frequency metrology, we typically use an intracavity gas pressure of 1–10 mTorr (1 Torr = 133 Pa). For the 3-mTorr sample gas, we measured its linear absorption through our 46.9-cm-long cavity (single pass) to be 6×10^{-7}, which leads to an absorption coefficient of 4.3×10^{-6}/Torr cm. The present cavity has a resonant transmission efficiency of 20%, which is decreased by 5.8×10^{-3} near the Doppler profile peak (a contrast of 2.9%). For sub-Doppler resolution, we use an incident power of 0.45 mW, and the cavity builds up the power to 3.2 W inside, with 90 μW available in the transmission. The saturated absorption resonance is obtained with a saturation parameter S of ~0.6. One obtains the linewidth of the molecular transition by taking the sum of the transit time- and the collision-broadening factors and multiplying this sum by the power-broadening factor. (The natural linewidth associated with a vibrational transition is of the order of 1 kHz.) The transit time limited free-flight linewidth is 270 kHz, dictated by the cavity beam waist of 410 μm. The pressure-broadening rate, measured for another overtone transition of acetylene,[6] is ~30 kHz/mTorr. The saturation parameter can be deduced from either the linewidth broadening ($\sqrt{1+S}$) or the growth of the saturation hole contrast ($1/\sqrt{1+S} - 1/\sqrt{1+2S}$) with respect to intracavity power.

One of the most sensitive techniques for absorption measurement has been developed in our previous research of noise-immune cavity-enhanced optical heterodyne molecular spectroscopy (NICE-OHMS).[6] We combine the FM spectroscopy with the cavity enhancement technique in the following way: The input laser beam is frequency modulated at exactly the cavity free spectral range (see EOM 2 in Fig. 1). The light transmitted through an empty cavity preserves its pure FM characteristic, and its heterodyne detection (by a resonant photodetector, labeled PD 2 in Fig. 1) is insensitive to any (small) relative frequency noise between the laser and the cavity. A useful signal is produced when one of the FM components is phase shifted or attenuated by the intracavity molecular dispersion and absorption. To further suppress the noise in this high-frequency modulation–demodulation channel, we dither the cavity length (200 kHz peak to peak) at a low audio frequency, and we use a lock-in amplifier to detect the signal following the high-frequency rf demodulation. The line shape of the recovered signal follows the modulation-broadened derivative of the dispersion.[12] Figure 5(a) shows a representative trace of the demodulated signal, obtained by use of an averaging time constant of 50 ms, with the operational parameters listed above. The signal has a FWHM of ~500 kHz, which includes the dither contribution. With the saturated absorption level estimated at 68×10^{-9}, the obtained S/N ratio normalized to 1 s is 940, leading to a noise-equivalent detection sensitivity of 7×10^{-11} of the integrated absorption. This result is ~13 times above the calculated shot-noise limit.[6]

To stabilize the cavity length on the molecular transition, we first need to obtain an adequate antisymmetric discrimination line shape by using the second-harmonic detection from the lock-in amplifier. The resultant molecular error signal is shown in Fig. 5(b). The error signal goes through a servo loop filter and reaches the PZT driver that controls the cavity length. The quality of this signal sets the frequency standard deviation of the laser–cavity system within the molecular servo bandwidth. Clearly, this bandwidth needs to remain low because of the finite S/N ratio of the molecular signal. We do not

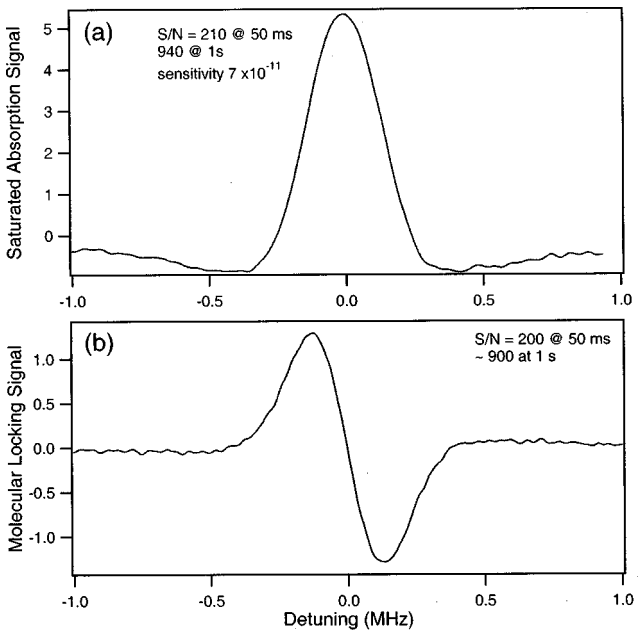

Fig. 5. (a) Intracavity saturated absorption signal of C_2H_2 $(3\nu_3)$ $R(29)$ transition at 1031.653 nm, with 3-mTorr sample gas; saturated absorption, 0.07 ppm; FWHM ~500 kHz. The detection sensitivity normalized to 1 s is 6.4×10^{-11} of the integrated absorption. (b) Antisymmetric error signal derived from the same molecular transition that is used to stabilized the laser–cavity system.

want excessive measurement noise to be written back onto the laser–cavity system. In the following discussion we present a guideline for setting an appropriate molecular servo bandwidth.

Suppose the molecular resonance has a HWHM linewidth of $\Delta\nu_{\text{mole}}$, and it is recovered with a S/N ratio of $(S/N)_{1s}$ at 1 s. If we use a servo loop bandwidth of B to process this signal, in an ideal servo system the measurement noise would be converted to the laser frequency noise according to

$$\Delta f_{\text{rms}} = \frac{\Delta\nu_{\text{mole}}}{(S/N)_{1s}}\sqrt{2\pi B}. \tag{2}$$

This rms frequency noise should be kept smaller than the rms linewidth δf_{laser} of the cavity-stabilized laser, which is determined mainly by the vibration and drift of the reference cavity itself. Hence

$$\Delta f_{\text{rms}} = \frac{\Delta\nu_{\text{mole}}}{(S/N)_{1s}}\sqrt{2\pi B} < \delta f_{\text{laser}},$$

$$\therefore\ B < \frac{1}{2\pi}\left[(S/N)_{1s}\frac{\delta f_{\text{laser}}}{\Delta\nu_{\text{mole}}}\right]^2. \tag{3}$$

In our case the molecular HWHM linewidth is ~250 kHz, and we have a S/N ratio of 900 at 1 s for this signal. The cavity-stabilized laser has a rms linewidth of ~1 kHz owing to the cavity vibration, so the maximum bandwidth for the molecular servo loop is limited to ~2 Hz. The simple procedure presented above is basically equivalent to the approach of comparing the Allan deviation of the prestabilized laser with the calculated Allan deviation obtainable with the lock to the molecular line. The cross point of the two deviation curves is the usual choice of the attack time of the molecular locking servo. After all, the whole purpose of this slow servo loop is to maintain the long-term stability of the laser frequency. After stabilizing the cavity length to the molecular transition we confirm that, as shown in Fig. 3, the rising Allan variance of the AOM–VCO does not change when the laser is locked on the cavity, thus confirming that the drift is due mainly to the laser itself.

In conclusion, we have successfully stabilized a diode-pumped Yb:YAG laser with a high-finesse optical cavity, which is subsequently stabilized by a sub-Doppler molecular transition. Using submilliwatt optical power, we have achieved a detection sensitivity of 7×10^{-11} at a 1-s averaging time. We are working toward construction of a second such system so that heterodyne comparison between the two systems would permit us to perform systematic studies of this stabilization scheme.

ACKNOWLEDGMENTS

Portions of this work were performed under a Cooperative Research and Development Agreement between National Institute of Standards and Technology (NIST) and Coherent Technologies, Inc. The work at JILA is supported by NIST and by the National Science Foundation.

*Permanent address, East China Normal University, Shanghai 200062, China.

J. Ye can be reached by e-mail at ye@jila.colorado.edu.

REFERENCES

1. T. Y. Fan, "Heat generation in Nd:YAG and Yb:YAG," IEEE J. Quantum Electron. **29**, 1457–1459 (1993).
2. C. Hönninger, G. Zhang, U. Keller, and A. Giesen, "Femtosecond Yb:YAG laser using semiconductor saturable absorbers," Opt. Lett. **20**, 2402–2404 (1995).
3. T. J. Carrig, J. W. Hobbs, C. J. Urbina, G. J. Wagner, C. P. Hale, S. W. Henderson, R. A. Swirbalus, and C. A. Denman, "Single-frequency, diode-pumped Yb:YAG and Yb:YLF lasers," in *Advanced Solid-State Lasers*, H. Injeyan, U. Keller, and C. Marshall, eds., Vol. 34 of OSA Trends in Optics and Photonics Series (Optical Society of America, Washington, D.C., 2000), paper WC12.
4. J. L. Hall and T. W. Hänsch, "External dye-laser frequency stabilizer," Opt. Lett. **9**, 502–504 (1984).
5. R. W. P. Drever, J. L. Hall, F. V. Kowalski, J. Hough, G. M. Ford, A. J. Munley, and H. Ward, "Laser phase and frequency stabilization using an optical resonator," Appl. Phys. B **31**, 97–105 (1983).
6. J. Ye, L.-S. Ma, and J. L. Hall, "Ultrastable optical frequency reference at 1.064 μm using a C_2HD molecular overtone transition," IEEE Trans. Instrum. Meas. **46**, 178–182 (1997); J. Ye, L.-S. Ma, and J. L. Hall, "Ultrasensitive detections in atomic and molecular physics: demonstration in molecular overtone spectroscopy," J. Opt. Soc. Am. B **15**, 6–15 (1998).
7. J. Ye and J. L. Hall, "Optical phase locking in the microradian domain: potential applications to NASA spaceborne optical measurements," Opt. Lett. **24**, 1838–1840 (1999).
8. D. S. Elliot, R. Roy, and S. J. Smith, "Extracavity laser band-shape and bandwidth modification," Phys. Rev. A **26**, 12–18 (1982).
9. D. Hils and J. L. Hall, "Ultrastable cavity-stabilized lasers with sub-Hertz line width," in *Proceedings of the Fourth International Symposium on Frequency Standards and Metrology*, A. De Marchi, ed. (Springer-Verlag, Heidelberg, 1989), pp. 162–173.
10. J. L. Hall designed and tested this driver in 1997 at JILA.
11. M. Herman, T. R. Huet, and M. Vervloet, "Spectroscopy and vibrational couplings in the $3\nu_3$ region of acetylene," Mol. Phys. **66**, 333–353 (1989).
12. R. L. Smith, "Practical solutions of the lock-in detection problem for Lorentz and dispersion resonance signals," J. Opt. Soc. Am. **61**, 1015–1022 (1971).